

Spin State, Structure, and Reactivity of Terminal Oxo and Dioxygen Complexes of the (PNP)Rh Moiety

Alexander Y. Verat, Hongjun Fan, Maren Pink, Y.-S. Chen, and Kenneth G. Caulton*^[a]

Abstract: [Rh^{III}H]({tBu₂PCH₂SiMe₂-NSiMe₂CH₂PtBu{CMe₂CH₂})), ([RhH-(PNP*)]), reacts with O₂ in the time taken to mix the reagents to form a 1:1 η²-O₂ adduct, for which O–O bond length is discussed with reference to the reducing power of [RhH(PNP*)]; DFT calculations faithfully replicate the observed O–O distance, and are used to understand the oxidation state

of this coordinated O₂. The reactivity of [Rh(O₂)(PNP)] towards H₂, CO, N₂, and O₂ is tested and compared to the associated DFT reaction energies. Three different reagents effect single

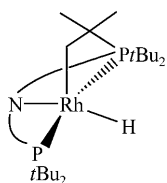
Keywords: C–H activation • dioxygen ligands • nitrous oxide • oxo ligands • rhodium

oxygen atom transfer to [RhH(PNP*)]. The resulting [RhO(PNP)], characterized at and above –60 °C and by DFT calculations, is a ground-state triplet, is nonplanar, and reacts, above about +15 °C, with its own *t*Bu C–H bond, to cleanly form a diamagnetic complex, [Rh(OH){N(SiMe₂CH₂PtBu₂)(SiMe₂-CH₂PtBu{CMe₂CH₂})}].

Introduction

The reducing power (and π-basicity) of any Rh compound is anticipated to be less than that of its Ir analogue. This is true of ν_{CO} values for [M(CO)(PNP)]^[1] for Rh and Ir respectively (PNP^[2] = {tBu₂PCH₂SiMe₂NSiMe₂CH₂PtBu(CMe₂CH₂)}). Surprisingly, data has been presented^[1] showing that the (PNP)Rh moiety is a weaker π-base than its cobalt analogue. Where does that leave (PNP)Rh, on an absolute scale? [RhH₂(PNP)] is a dihydride, hence Rh^{III}, but oxidative addition of benzene to give [RhH(C₆H₅)(PNP)], although it is observed, has Δ*G*^o ≈ 0. We have shown that^[3] three-coordinate [Rh(PNP)]

has a ground-state structure with one *t*Bu methyl group oxidatively added to Rh^I, to yield the structure [Rh^{III}H-*t*Bu₂PCH₂SiMe₂NSiMe₂CH₂PtBu(CMe₂CH₂)]}. Moreover, photoproducted authentic three coordinate [Rh^I(PNP)] oxida-



tively adds that H–C(sp³) bond on the nanosecond time-scale.^[4]

Species of formula [Rh(O_n)(PNP)] where *n* = 2 and 1, are clearly relevant to the reducing power of [Rh^{III}H-*t*Bu₂PCH₂SiMe₂NSiMe₂CH₂PtBu(CMe₂CH₂)]}. Complexes containing η¹ or η² O₂ are quite common among the transition metals, yet utilizing their residual oxidizing power remains challenging. In contrast, terminal oxo ligands on metals containing six or more d electrons are very rare,^[5–11] for reasons that have been analyzed;^[12] they are expected to be highly nucleophilic, and thus perhaps not oxidizing. Synthesis of such terminal oxo complexes with “high” d-electron counts would help test these predictions, and constitutes part of what is reported here.

Results

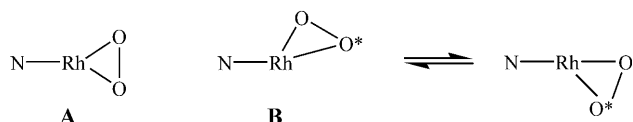
An interesting molecule has been reported^[13] recently: [Rh(η²-O₂){Me₂C₆H(CH₂PtBu₂)₂}]}. It was synthesized from a source of Rh^I and O₂, and was said to be remarkable in that the O–O distance (1.36 Å) was shorter than in many other structurally characterized Rh–O₂ complexes. Moreover, given the evidence that the O–O bond lengthens along the series O₂, O₂¹⁻, O₂²⁻ (i.e. as O–O bond order decreases), the interpretation derived^[13] from the structural data was that [Rh(η²-O₂){Me₂C₆H(CH₂PtBu₂)₂}] is a complex of neutral dioxygen bound to Rh^I. This would be a remarkable resistance to oxidation by an otherwise reducing (pincer)Rh fragment.

[a] A. Y. Verat, H. Fan, M. Pink, Y.-S. Chen, Prof. K. G. Caulton
Department of Chemistry, Indiana University, Bloomington, IN
and Argonne National Laboratory, Argonne IL (USA)
Fax: (+1) 812-855-8300
E-mail: caulton@indiana.edu

Supporting information for this article is available on the WWW
under <http://dx.doi.org/10.1002/chem.200800573>.

Indeed, molecular oxygen appears to *lack* pure σ -donor power, in the absence of electron transfer to O_2 , by virtue of not complexing to any non-redox active Lewis acid, for example, d^0 (TiCl₄) or even d^9 (Cu^{II}) or d^{10} (Zn^{II}).

We report here that the C–H bond-cleaved pincer complex $[Rh^{III}H\{tBu_2PCH_2SiMe_2NSiMe_2CH_2PtBu(CMe_2CH_2)\}]$,^[3] is converted cleanly and completely by O_2 to form $[Rh(O_2)(PNP)]$, in which PNP is intact $(tBu_2PCH_2SiMe_2)_2N$. This molecule has ³¹P and ¹H NMR spectra consistent with a C_{2v} structure (**A**), although structure **B** (C_s symmetry) might be fluxional, and thus show time-averaged C_{2v} symmetry.



The observed J_{PRh} value in the ³¹P NMR spectrum, 123 Hz, is not very close to that^[13] in $[Rh(\eta^2-O_2)\{Me_2C_6H(CH_2PtBu_2)_2\}]$, 146 Hz. Although there is a general trend that J_{PRh} is “smaller” for Rh^{III} than for Rh^I, the generality of this criterion has been questioned.^[14]

The single-crystal structure (Figure 1) of $[Rh(O_2)(PNP)]$ shows it to be close to C_{2v} symmetric. The unit cell contains

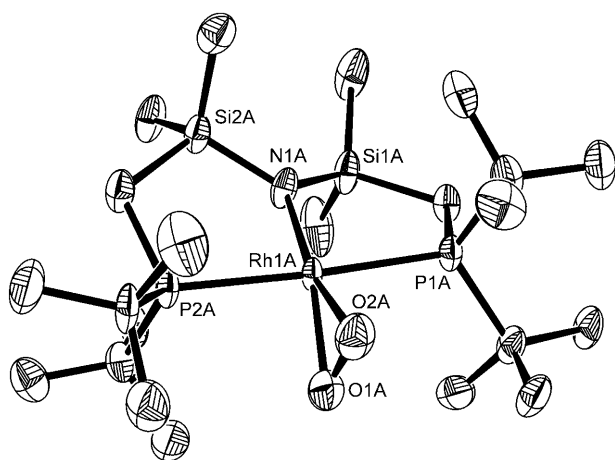


Figure 1. ORTEP drawing (50% probability) of the non-hydrogen atoms of $[Rh(O_2)(tBu_2PCH_2SiMe_2)_2N]$. Unlabelled atoms are carbon.

two crystallographically independent molecules, but Table 1 shows that the two are identical, even down to small details (see also the least squares fit in the Supporting Information). The structure is very faithful to C_2 symmetry and both Rh–O and O–O distances are nearly identical to those of $[Rh(\eta^2-O_2)\{Me_2C_6H(CH_2PtBu_2)_2\}]$. The bite angle of the PNP ligand makes the $\angle P-Rh-P$ about 11° larger than that of the PCP analogue. The Rh–O distances are shorter than those in many higher coordination number RhO_2 complexes, but higher coordination number always lengthens metal–ligand bonds. In summary, this new structure also shows the

Table 1. Selected bond lengths [\AA] and angles [$^\circ$] for $[Rh(O_2)(PNP)]$.

	Molecule A	Molecule B
O1–O2	1.363(10)	1.356(11)
Rh1–N1	2.019(7)	2.004(7)
Rh1–O1	2.011(7)	1.998(8)
Rh1–O2	2.024(7)	2.019(7)
Rh1–P1	2.355(2)	2.363(3)
Rh1–P2	2.352(2)	2.364(3)
N1–Rh1–O2	161.5(3)	161.8(4)
N1–Rh1–P1	88.2(2)	89.0(2)
N1–Rh1–P2	88.6(2)	88.4(2)
O1–Rh1–N1	159.0(4)	158.8(4)
O1–Rh1–P1	96.6(2)	96.3(3)
O1–Rh1–P2	86.8(2)	86.3(3)
O2–Rh1–P1	86.8(2)	86.6(3)
O2–Rh1–P2	95.9(2)	95.6(3)
P1–Rh1–P2	176.57(10)	177.35(10)

“short” 1.36 \AA O–O distance reported for the PCP analogue. Although a number of the longer (1.41–1.47 \AA) values quoted for RhO_2 complexes were determined prior to 1976, and at 25 $^\circ\text{C}$, there is no evidence that higher thermal motion, and possible disorder are at fault here.^[15] Previous work cited a range of O_2 complexes of d^6 – d^{10} metals (Ru, Os, Pd, Ir), which have O–O distances in the range 1.30–1.37 \AA . Thus, perhaps this parameter is not truly reliable for establishing charge state, but rather only the degree of back bonding.

Figure 2 shows a scatter plot of crystallographically determined O–O distances for transition metal complexes $[M(\eta^2-$

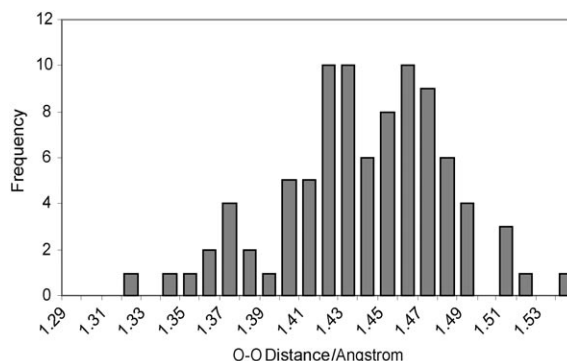


Figure 2. Scatter plot of O–O distances from Cambridge Crystallographic Database on $[M(\eta^2-O_2)]$ complexes.

O_2]; this reveals that distances shorter than 1.36 \AA are very rare (only single examples, and some of these have been shown^[15] to involve static or dynamic disorder), so the cause of the present short distances remains to be determined. A consideration of compounds with distances below about 1.4 \AA shows them to involve either unsaturated species or relatively poor donors, or π -acid ligands, all of which diminish the reducing power of the metal. For example, a molecule^[16] closely related to $[Rh(O_2)(PCP)]$, but with one additional donor ligand (hence saturated Rh) has an O–O distance of 1.434(3) \AA .

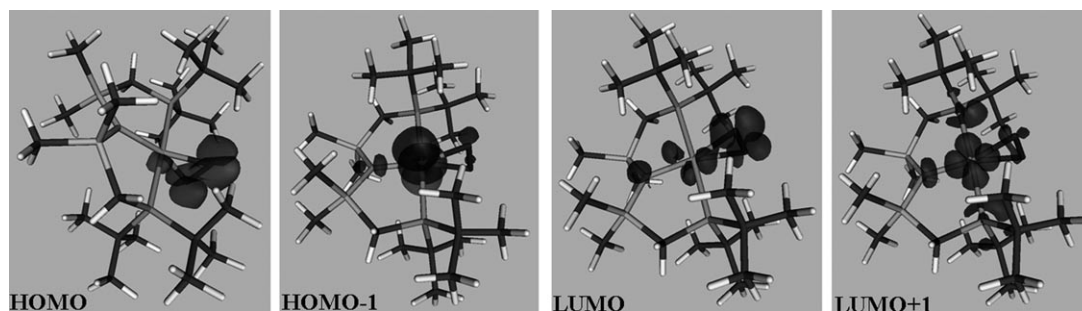


Figure 3. Frontier orbitals of $[\text{Rh}(\text{O}_2)(\text{PNP})]$. For color, see the Supporting Information.

DFT computational analysis: DFT (B3LYP) calculations on the complete species $[\text{Rh}(\text{O}_2)\{\text{tBu}_2\text{PCH}_2\text{SiMe}_2\text{N}\}]$ gave an optimized structure, which had no significant differences from experiment, including the calculated O–O distance, 1.38 Å, confirming that the experimental measurement 1.36 Å is not in question. It thus appears that the dominant factor limiting back bonding/reduction of O_2 in $[\text{Rh}(\text{O}_2)(\text{PNP})]$ is the unsaturated character of the molecule, irrespective of the π -donor amide and the initial d^8 configuration of the metal: unsaturation leaves the $\text{Rh}(\text{PNP})$ fragment less capable of back bonding to the arriving O_2 reagent than if the species were saturated.

The frontier orbitals (Figure 3) show the HOMO to be $\pi_{\text{O}_2}^*$, and relatively unmixed, due to its poor overlap (δ symmetry) with metal orbitals. The calculated electronic energy for binding O_2 to three coordinate $\text{Rh}(\text{PNP})$ is $-40.3 \text{ kcal mol}^{-1}$.

To test the hypothesis that 16-valence-electron O_2 complexes have less back donation to O_2 , we compared the minimum energy structures of $[\text{Rh}(\text{O}_2)(\text{PNP})]$ to those of $[\text{RhL}(\text{O}_2)(\text{PNP})]$, in which L is NH_3 , and also the stronger donor 4-Me₂N-pyridine. The structures for the two different L ligands differ insignificantly,^[17] showing that the mere presence of a donor is more influential than its specific donor power. Both adducts show an O–O distance lengthened by 0.03 Å, which puts it (1.41 Å) in the range of crystallographic determinations of $\text{M}(\eta^2\text{-peroxide})$ species (Figure 2). There is a huge (0.22 Å) lengthening of the Rh–NSi₂ distance on binding L, which supports the idea that amide acts as a π -donor in $[\text{Rh}(\text{O}_2)(\text{PNP})]$ itself, and that the LUMO of $[\text{Rh}(\text{O}_2)(\text{PNP})]$ has π_{RhN}^* character. In contrast, binding L to $[\text{Rh}(\text{O}_2)(\text{PNP})]$ does not significantly lengthen the Rh–O distance.

Reactivity studies: If $[\text{Rh}(\text{O}_2)(\text{PNP})]$ were composed of Rh^{I} (PNP) and singlet O_2 η^2 bonded to the metal, then it should contain latent reducing equivalents. To test this, we have recorded the ^1H and ^{31}P NMR spectra of $[\text{Rh}(\text{O}_2)(\text{PNP})]$ under 1 atm of O_2 in $[\text{D}_8]$ toluene saturated at -60°C ; no new species, specifically no 18-valence-electron adduct $[\text{Rh}(\text{O}_2)_2(\text{PNP})]$ was produced. It is of course also of interest that this molecule does not spontaneously rearrange to $[\text{Rh}^{\text{I}}\{\text{N}(\text{SiMe}_2\text{CH}_2\text{P}t\text{Bu}_2=\text{O})\}_2]$, by oxidation of both P^{III} atoms. In fact, the DFT (B3LYP) energy for the conversion

of the obtained complex to this bis-phosphine oxide product is favorable (by $65.4 \text{ kcal mol}^{-1}$), so the obtained product is a kinetic, but not the thermodynamic product. It is interesting that complete utilization of the oxidizing equivalents of O_2 on phosphorus is thermodynamically preferred, in spite of this forming planar, 3-coordinate and monovalent rhodium.

The reactivity of $[\text{Rh}(\text{O}_2)(\text{PNP})]$ was further tested, in an effort to probe for redox equivalents available at Rh and/or at O_2 .

a) N_2 : A benzene solution of $[\text{Rh}(\text{O}_2)(\text{PNP})]$ was shaken constantly at 23°C in the presence of 1 atm of N_2 for 21 h. There was absolutely no change. Consistent with this observation, the calculated DFT reaction electronic energy for this reaction is $+10.6 \text{ kcal mol}^{-1}$.

b) CO : A benzene solution of $[\text{Rh}(\text{O}_2)(\text{PNP})]$ was shaken in the presence of 1 atm of CO for 5 min. There was essentially complete conversion to the known^[1] $[\text{Rh}(\text{CO})(\text{PNP})]$, with concurrent disappearance of $[\text{Rh}(\text{O}_2)(\text{PNP})]$. The fate of the O_2 , which could be either liberation as the free diatomic or oxidative removal as CO_2 , was evident because the reaction, even when run with a 1:1 molar stoichiometry, gave complete consumption of $[\text{Rh}(\text{O}_2)(\text{PNP})]$, indicating that the two “extra” CO , which are required to make CO_2 , were unnecessary. The calculated DFT reaction electronic energies for these two different reactions are -16.0 (formation of O_2) and -158.7 (formation of 2CO_2) kcal mol^{-1} . This indicates that $[\text{Rh}(\text{CO})(\text{PNP})]$ is in fact thermodynamically somewhat immune to decomposition by O_2 since the latter is a product of this reaction.

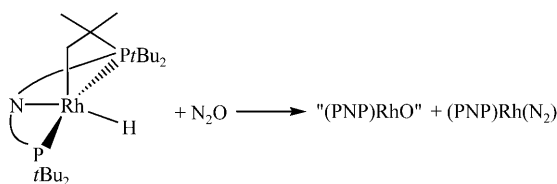
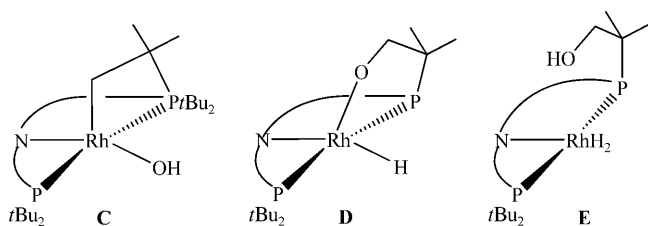
c) H_2 : A benzene solution of $[\text{Rh}(\text{O}_2)(\text{PNP})]$ was shaken constantly in the presence of 1 atm of H_2 and periodically monitored from 20 min to 40 h. There was progressive growth of $[\text{Rh}(\text{H})_2(\text{PNP})]$, with concurrent decrease of $[\text{Rh}(\text{O}_2)(\text{PNP})]$. At 20 h, the reaction had consumed essentially all $[\text{Rh}(\text{O}_2)(\text{PNP})]$. The fate of the O_2 , which could be either liberation as the free diatomic or conversion to H_2O or H_2O_2 , was investigated by ^1H NMR. This showed no signal for the acidic protons of water (near 1 ppm in benzene); however, the fact that there was slow degradation to an Rh-free organophosphorus compound, which could be

due either to oxidation of P atoms or of hydrolysis of Si–N bonds, prevents any definitive conclusion on the fate of the former O₂ ligand. The calculated DFT reaction electronic energies for these two different reactions are +8.4 (producing O₂) versus –106.7 (producing H₂O) kcal mol^{–1}; hence water production significantly aids the thermodynamics, in spite of the associated entropy penalty.

In summary, the O₂ complex is reactive, and not only with oxidants, which might have been expected if it were^[13] Rh^I, but these reactivity results do not strongly point to any particular oxidation state of the Rh in [Rh(O₂)(PNP)]. Rather, they reflect reaction thermodynamics, which can be favorable not only with oxidants, but also simply with “good ligands.” Certainly there is good evidence^[18,19] that CO is a better ligand (thermodynamically) than H₂ or most other ligands, but its strength relative to O₂ has not been previously established. Moreover, we deal here with Rh, which has significantly less favorable redox reaction enthalpies than, for example, the more reducing Ir.

Deoxygenation of N₂O by [Rh^{III}H(*t*Bu₂PCH₂SiMe₂NSiMe₂CH₂PrBu(CMe₂CH₂))]:

a) Product characterization: [Rh^{III}H(*t*Bu₂PCH₂SiMe₂NSiMe₂CH₂PrBu(CMe₂CH₂))] has an oxidation state of Rh that does not clearly qualify it to function as a reducing agent. In fact, [Rh^{III}H(*t*Bu₂PCH₂SiMe₂NSiMe₂CH₂PrBu(CMe₂CH₂))] reacts with N₂O (1 atm, 3.6 equiv) at 23 °C in benzene to form a 1:1 stoichiometry of the known^[3] [Rh(N₂)(PNP)] together with a diamagnetic molecule of C₁ symmetry, in which the ³¹P{¹H} NMR spectrum has an AMX pattern (X = Rh); the J_{AM} value, 442 Hz, indicates a mutually *trans* location of the P_A and P_M nuclei, and coupling constants to the Rh atom of a magnitude 108 and 82 Hz are indicative of direct Rh–P bonds. The ¹H NMR spectrum of this diamagnetic product shows three *t*Bu doublets and two single methyl doublets, consistent with functionalization of one *t*Bu group; the molecule also shows a unit intensity doublet of doublets at δ = –3.0 ppm (assigned below), with this



spin coupling (J_{PH}) confirming the non-equivalence of the two phosphorus nuclei.

We envisioned two possible ways to make the P nuclei nonequivalent, with structures **C** and **D**. Late transition metal bonds to oxygen are generally subject to hydrogenolysis, to replace O ligands on the metal by hydride. If the structure were **C**, hydrogenolysis would form [RhH₂(PNP)] and water. If it were **D**, the O–C bond is unreactive and so the product would be **E**, with one phosphorus irreversibly rendered nonequivalent to the other. In fact, treatment of the AMX compound with 1 atm H₂ in THF gives, after 12 h at 23 °C, complete conversion to [RhH₂(PNP)], consistent with **C**, [Rh(OH){N(SiMe₂CH₂PrBu₂)(SiMe₂CH₂PrBu{CMe₂CH₂})}], as the product of intramolecular attack of the terminal oxo ligand on the methyl group. We attribute the ¹H NMR signal at δ = –3.0 ppm to the hydroxyl proton in **C**; there is precedent for hydroxyl protons with negative chemical shifts, and for three bond coupling to P^[20–22] Also, the unusually large observed J_{pp} value (442 Hz) is attributed to it involving one P atom in a small ring in **C**.

b) Detection of an intermediate: Combining N₂O and [Rh^{III}H(*t*Bu₂PCH₂SiMe₂NSiMe₂CH₂PrBu(CMe₂CH₂))] (1:1 mole ratio) at –78 °C in [D₈]toluene and mixing with minimal warming above that temperature, then recording ¹H and ³¹P NMR spectra starting at –60 °C reproducibly shows essentially complete consumption of [Rh^{III}H(*t*Bu₂PCH₂SiMe₂NSiMe₂CH₂PrBu(CMe₂CH₂))] and production of the known [Rh(N₂)(PNP)], together with three ¹H NMR signals due to a C_{2v} symmetric, paramagnetic (*t*Bu at δ = 19.1 ppm, SiMe at δ = –2.1 ppm, and SiCH₂P at δ = –8.6 ppm) co-product. Chemical shifts are noticeably temperature dependent, consistent with paramagnetism. There are no ³¹P or ¹H NMR signals due to the AMX product **C** at this temperature. This paramagnetic co-product disappears on warming to 23 °C, concurrent with the appearance of the AMX ³¹P{¹H} NMR pattern described above, due to **C**.^[23]

DFT (B3LYP) calculations of candidate intermediates in the early stages of reaction^[17] show that 1:1 adducts formed by binding the triatomic molecule through the O atom or the N=O bond (η^2) are energetically inferior to binding through only the terminal N atom (most stable of all), or η^2 coordination to the N=N bond. Both have pendant oxygen.

The local concentrations in this reaction are such that [Rh(N₂O)(PNP)] will encounter a second molecule of [Rh^{III}H(*t*Bu₂PCH₂SiMe₂NSiMe₂CH₂PrBu{CMe₂CH₂})], with the result that O-atom transfer is the most probable second mechanistic step, yielding [Rh(N₂)(PNP)] and [RhO(PNP)]. The experimental observations (³¹P, none, and ¹H NMR spectroscopy) together suggest that [RhO(PNP)] is paramagnetic. DFT (B3LYP) calculations of singlet and triplet [RhO(PNP)] show the latter to be more stable (by 15.3 kcal mol^{–1}), and to have a planar geometry, with a Rh–O distance of 1.81 Å. Triplet spin densities are 0.92 on the Rh (mainly the xy orbital, α_{136} in Figure 4), 0.08 on the N and 0.96 on the O atom, showing this triplet to have O-centered radical character. The spin density at the amide N atom

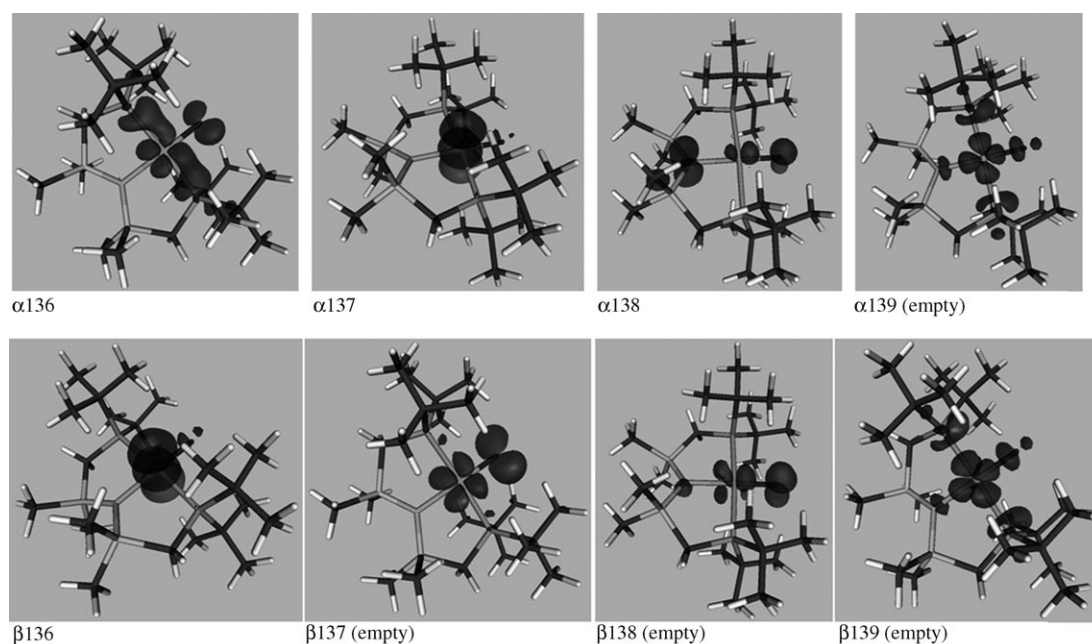


Figure 4. Frontier orbitals of triplet [RhO(PNP)]. For color, see the Supporting Information.

comes from frontier orbital $\alpha 138$ (Figure 4), which also involves the d_{yz} orbital and one oxygen p_{π} orbital; it makes the oxo ligand electrophilic. These two frontier orbitals are π^*_{RhO} in character; they thus contribute to reduction of the Rh–O bond order. Another feature of the triplet is that its Rh–N distance is 0.08 Å longer than its singlet; this is consistent with singly populating the yz orbital, which is π^*_{RhN} . This means there is radical character primarily at Rh and at the oxo ligand, thus preparing it for C–H bond cleavage by this Rh–O diradical. The frontier orbitals of triplet [RhO(PNP)] show (Figure 4 and the Supporting Information) x^2-y^2 to be unoccupied (α and β 139); consistent with the d-orbital splitting pattern of planar complexes, that orbital is strongly σ^* .

Because the H–C(sp^3) cleavage reaction of [RhO(PNP)] begins in the triplet state, we begin our analysis on that reaction path, with the understanding that the later minimum energy crossing point,^[24,25] where a singlet forms, may involve very different geometry and frontier orbitals. We therefore seek an empty orbital of triplet [RhO(PNP)] for interacting with the electron density of a C–H bond. As shown in Figure 4, only α and β 139 are completely empty (each has some oxo character), but both lie in the P_2NRh coordination plane. β 137 and β 138, two orthogonal π^*_{RhO} orbitals, are perhaps better candidates, the latter being directed perpendicular to the P_2NRhO plane, where the *t*Bu groups are found. As an agostic interaction there progresses to weaken the Rh–O bond (by filling the π^*_{RhO}), a single bond develops to form the hydroxyl ligand (and Rh–C(sp^3) bond). Note that, since the final product is expected to be a square pyramid with the CH_2 -substituent apical, \angle N–Rh–O will be nearly constant in the range $180^\circ \rightarrow 165^\circ$ throughout the C–H cleavage mechanism; this increases the validity

of an analysis that uses the ground-state triplet frontier orbitals and structure.

Alternative O-atom transfers: Reaction of [Rh^{III}H(*t*Bu₂PCH₂SiMe₂NSiMe₂CH₂P*t*Bu(CMe₂CH₂))] with excess pyridine *N*-oxide in THF at 25 °C gives immediate conversion to equimolar [Rh(pyridine)(PNP)] and the same AMX product, **C**, described above. Likewise, [Rh^{III}H(*t*Bu₂PCH₂SiMe₂NSiMe₂CH₂P*t*Bu(CMe₂CH₂))] is converted to the same AMX product by an equimolar amount of Me₃NO in THF in the time taken to mix the reagents at 25 °C. Released Me₃N and excess Me₃NO are readily removed by filtration and drying in vacuum. Once formed by these methods, the AMX compound is stable in hydrocarbon solvent for at least 4 h.

Conclusion

The finding that d^6 [RhO(PNP)] can be produced in a kinetically facile reaction and that the same species is produced by three different O-atom transfer reagents, is informative on the identity of such a species. The triplet ground state is not predictable from first principles, but [RhO(PNP)] needs to be recognized as isoelectronic with d^6 [RuCl(PNP)], which also has a planar triplet ground state.^[26] Both of these arise since the two frontier orbitals, one that bonds poorly to ligands and the other that is π^* with respect to the amide nitrogen, are nearly degenerate, so that a triplet spin state is favored. The related species^[27] [RuN(PNP)], being d^4 , does not have this spin-state option.

The triplet character of [RhO(PNP)] means that the mechanism of cleavage of an H–C(sp^3) bond needs to be

considered not only as a two-electron process (see above at the early stage of H–C cleavage) but also possibly stepwise, with a later geminate carbon and Rh-centered diradical intermediate. However, the metal oxidation state is unchanged in this reaction. The high reactivity of such a terminal oxo species is clearly demonstrated here, as is the selectivity (due to the more isotropic character of an alkyl H) to transfer H atoms from oxygen and carbon to Rh in the product; the unusual chemical shift of late transition metal hydroxides makes it possible to misidentify this as a hydride complex.

Experimental Section

General procedures: All reactions were performed in a glove box or on a Schlenk line by using standard air-sensitive techniques. Solvent distillation was carried out by using either Na/benzophenone or CaH₂, or with a Grubbs-type purification system or a combination of these. They were degassed and stored in air-tight glassware. [Rh^{III}H{tBu₂PCH₂SiMe₂NSiMe₂CH₂PrBu(CMe₂CH₂)}] was prepared by following the published synthesis.^[1] ¹H NMR chemical shifts are reported in ppm relative to protio impurities in the deuterated solvents. ³¹P{¹H} spectra are referenced to external standards of 85% H₃PO₄ (at 0 ppm). NMR spectra were recorded with a Varian Gemini 2000 (300 MHz ¹H; 121.5 MHz ³¹P), or a Varian Inova instrument (400 MHz ¹H; 162 MHz ³¹P). Gas reactions were carried out on a calibrated gas line with the solution being first degassed and 2.2 mL of headspace assumed for the NMR tube. ESI mass-spectra were recorded on a PE-Sciex API III Triple Quadrupole mass spectrometer in THF solutions.

Synthesis of [Rh(O₂)(PNP)]: [Rh^{III}H{tBu₂PCH₂SiMe₂NSiMe₂CH₂PrBu(CMe₂CH₂)}] (0.0115 g, 0.0208 mmol) was dissolved in C₆D₆ (0.6 mL) in a J-Young NMR tube. This solution was freeze-pump-thawed three times and O₂ (0.000668 g, 0.0208 mmol) was added from a gas line. The tube was shaken and an NMR spectrum was recorded. ³¹P{¹H} NMR (121.47 MHz, C₆D₆): δ = 48.29 ppm (d, ¹J_{PRh} = 122.9 Hz); ¹H NMR (300.07 MHz, C₆D₆): δ = 1.31 (vt, ³J_{HP} = 13.0 Hz, 36H, tBu), 0.71 (vt, ³J_{HP} = 9.0 Hz, 4H, Si-CH₂-P), 0.24 ppm (s, 12H, Si-CH₃). Crystals for X-ray analysis were obtained by slow evaporation of an Et₂O solution.^[28] Attempts to determine the ESI mass spectrum showed no molecular ion, even with addition of acetic acid.

Reaction of [Rh(O₂)(PNP)] with N₂: N₂ (1.3 atm) was added to a J-Young tube containing a solution of [Rh(O₂)(PNP)] in C₆D₆. After 21 h of end-over-end rotation [Rh(O₂)(PNP)] remains, and [RhN₂(PNP)] is not observed.

Reaction of [RhO₂(PNP)] with CO: To a J-Young tube containing a solution of [RhO₂(PNP)] in C₆D₆, 1 equiv of CO was added. After 5 min there was 95% conversion to [Rh(CO)(PNP)], with no other products observed.

Reaction of [Rh(O₂)(PNP)] with H₂: H₂ (1 atm) was added to a C₆D₆ solution of [Rh(O₂)(PNP)]. After 20 minutes of rotation, conversion to [RhH₂(PNP)] is 4%. After 8 h of rotation the ratio [RhH₂(PNP)]/[Rh(O₂)(PNP)] = 2:5, and after 19.5 h, 4:5. The tube was then freeze-pump-thawed three times, and hydrogen (1 atm) was re-applied. After 20 h of rotation the [Rh(O₂)(PNP)] had almost completely disappeared, but the ³¹P NMR spectrum showed an unidentified doublet at δ = 73.4 ppm (≈ 20%), and a singlet (hence no coordination to Rh) at δ = 58.5 ppm (≈ 15%), apparently a product from either released O₂ or H₂O. All other signals are due to [RhH₂(PNP)].

Reaction of Me₃NO with [Rh^{III}H{tBu₂PCH₂SiMe₂NSiMe₂CH₂PrBu(CMe₂CH₂)}]: Me₃NO (0.0026 g, 0.0346 mmol) was placed into a vial with [D₈]THF (1 mL). The contents of the vial were stirred for 5 minutes; not all Me₃NO dissolved. Then, [Rh^{III}H{tBu₂PCH₂SiMe₂NSiMe₂CH₂PrBu(CMe₂CH₂)}] (0.0190 g, 0.0346 mmol) was added and the solution was stirred for three minutes. The solution was filtered and after 5 minutes,

NMR spectra were recorded. ³¹P{¹H} NMR (161.98 MHz, [D₈]THF): δ = 39.36 (d, d, ¹J_{PRh} = 107.5 Hz, ²J_{PP} = 441.5 Hz, 1 P), 5.70 ppm (d, d, ¹J_{PRh} = 81.8 Hz, ²J_{PP} = 441.2 Hz, 1 P); ¹H NMR (400.12 MHz, C₆D₆): δ = 1.55 (d, ³J_{HP} = 13.0 Hz, 3H, CH₃ of activated tBu group), 1.42 (d, ³J_{HP} = 13.6 Hz, 9H, tBu), 1.28 (d, ³J_{HP} = 12.3 Hz, 9H, tBu), 1.26 (d, ³J_{HP} = 12.1 Hz, 9H, tBu), 1.15 (d, ³J_{HP} = 12.9 Hz, 3H, CH₃ of activated tBu group), 0.96 (d, ²J_{HP} = 10.3 Hz, 1H, P-CH), 0.91 (d, ²J_{HP} = 11.3 Hz, 1H, P-CH), 0.84 (d, ²J_{HP} = 9.2 Hz, 1H, P-CH), 0.80 (d, ²J_{HP} = 9.2 Hz, 1H, P-CH), 0.25 (s, 3H, Si-CH₃), 0.21 (s, 3H, Si-CH₃), 0.04 (s, 3H, Si-CH₃), 0.02 (s, 3H, Si-CH₃), -2.83 ppm (d, d, ³J_{HP} = 3.0 Hz, ³J_{HP} = 2.1 Hz, 1H, Rh-OH). Due to the large number of other signals, the signals of the RhCH₂ protons were not identified with certainty. The ¹H NMR also showed broad peaks of a paramagnetic species (δ 12.67, -4.15), attributed to [RhO(PNP)].

Reaction of pyridine N-oxide with [Rh^{III}H{tBu₂PCH₂SiMe₂NSiMe₂CH₂PrBu(CMe₂CH₂)}]: [Rh^{III}H{tBu₂PCH₂SiMe₂NSiMe₂CH₂PrBu(CMe₂CH₂)}] (0.0141 g, 0.0256 mmol) was dissolved in C₆D₆ (0.6 mL) in a J-Young NMR tube and pyridine N-oxide (0.0040 g, 0.042 mmol) was added. The tube was shaken for 10 minutes and ¹H and ³¹P NMR spectra were recorded. Spectra reveal formation of [Rh(PNP)(pyridine)] and **1**, [Rh(OH){N(SiMe₂CH₂PrBu₂)(SiMe₂CH₂PrBu(CMe₂CH₂))}], in the ratio of 1:1.

Reaction of N₂O with [Rh^{III}H{tBu₂PCH₂SiMe₂NSiMe₂CH₂PrBu(CMe₂CH₂)}]: a) At 25 °C: [Rh^{III}H{tBu₂PCH₂SiMe₂NSiMe₂CH₂PrBu(CMe₂CH₂)}] (0.0120 g, 0.0218 mmol) was dissolved in C₆D₆ (0.6 mL) in a J-Young NMR tube. This solution was freeze-pump-thawed three times and N₂O (1 atm) was added. ³¹P and ¹H NMR spectra recorded immediately showed formation of [Rh(N₂)(PNP)]. After one hour, ³¹P NMR shows formation of **1** and [Rh(OH){N(SiMe₂CH₂PrBu₂)(SiMe₂CH₂PrBu(CMe₂CH₂))}], in the ratio [RhN₂(PNP)]/**1** = 5:2.

b) *Variable-temperature reaction study:* Combining N₂O and [Rh^{III}H{tBu₂PCH₂SiMe₂NSiMe₂CH₂PrBu(CMe₂CH₂)}] (1:1 mole ratio) at and below -78 °C in [D₈]toluene was followed by recording ¹H and ³¹P NMR spectra at -60, -50, and -40 °C. This showed, already at -60 °C, complete consumption of [Rh^{III}H{tBu₂PCH₂SiMe₂NSiMe₂CH₂PrBu(CMe₂CH₂)}] and production of [RhN₂(PNP)]^[3] together with three ¹H NMR signals due to a C_{2v} symmetric, paramagnetic co-product (integrations at -60 °C correspond to the assignments tBu δ = 19.1 ppm, SiMe δ = -2.1 ppm, SiCH₂P δ = -8.6 ppm). These three chemical shifts are noticeably temperature dependent, moving towards the 0–10 ppm region upon warming, consistent with paramagnetism. There are no ³¹P or ¹H NMR signals due to the AMX product at this temperature, or until ≈ +15 °C. The paramagnetic product disappears completely on warming towards 23 °C, concurrent with increasing growth of the AMX ³¹P{¹H} NMR pattern described above from Me₃NO.

Acknowledgements

This work was supported by the National Science Foundation (NSF-CHE-0544829) and by the DOE under grant number CHE0087817, and by the DOE-BES under contract number W-31-109-Eng-38 at the Advanced Photon Source.

- [1] M. J. Ingleson, M. Pink, K. G. Caulton, *J. Am. Chem. Soc.* **2006**, *128*, 4248–4249.
- [2] M. D. Fryzuk, C. D. Montgomery, *Coord. Chem. Rev.* **1989**, *95*, 1–40.
- [3] A. Y. Verat, M. Pink, H. Fan, J. Tomaszewski, K. G. Caulton, *Organometallics* **2008**, *27*, 166–168.
- [4] R. D. Rimmer, D. C. Grills, H. Fan, P. C. Ford, K. G. Caulton, *J. Am. Chem. Soc.* **2007**, *129*, 15430–15431.
- [5] J.-U. Rohde, J.-H. In, M. H. Lim, W. W. Brennessel, M. R. Bukowski, A. Stubna, E. Muenck, W. Nam, L. Que, Jr., *Science* **2003**, *299*, 1037–1039.
- [6] J. M. Mayer, *Acc. Chem. Res.* **1998**, *31*, 441–450.

- [7] C. E. MacBeth, A. P. Golombek, V. G. Young, Jr., C. Yang, K. Kuczera, M. P. Hendrich, A. S. Borovik, *Science* **2000**, *289*, 938–941.
- [8] R. Gupta, A. S. Borovik, *J. Am. Chem. Soc.* **2003**, *125*, 13234–13242.
- [9] T. M. Anderson, R. Cao, E. Slonkina, B. Hedman, K. O. Hodgson, K. I. Hardcastle, W. A. Neiwert, S. Wu, M. L. Kirk, S. Knottenbelt, E. C. Depperman, B. Keita, L. Nadjo, D. G. Musaev, K. Morokuma, C. L. Hill, *J. Am. Chem. Soc.* **2008**, *130*, 2877.
- [10] R. Cao, T. M. Anderson, P. M. B. Piccoli, A. J. Schultz, T. F. Koetzle, Y. V. Geletii, E. Slonkina, B. Hedman, K. O. Hodgson, K. I. Hardcastle, X. Fang, M. L. Kirk, S. Knottenbelt, P. Koegerler, D. G. Musaev, K. Morokuma, M. Takahashi, C. L. Hill, *J. Am. Chem. Soc.* **2007**, *129*, 11118–11133.
- [11] T. M. Anderson, W. A. Neiwert, M. L. Kirk, P. M. B. Piccoli, A. J. Schultz, T. F. Koetzle, D. G. Musaev, K. Morokuma, R. Cao, C. L. Hill, *Science* **2004**, *306*, 2074–2077.
- [12] J. M. Mayer, *Comm. Inorg. Chem.* **1988**, *8*, 125–135.
- [13] C. M. Frech, L. J. W. Shimon, D. Milstein, *Helv. Chim. Acta* **2006**, *89*, 1730–1739.
- [14] M. C. Nicasio, M. Paneque, P. J. Perez, A. Pizzano, M. L. Poveda, L. Rey, S. Sirol, S. Taboada, M. Trujillo, A. Monge, C. Ruiz, E. Carmo, *Inorg. Chem.* **2000**, *39*, 180–188.
- [15] C. J. Cramer, W. B. Tolman, K. H. Theopold, A. L. Rheingold, *Proc. Natl. Acad. Sci. USA* **2003**, *100*, 3635–3640.
- [16] A. Vigalok, L. J. W. Shimon, D. Milstein, *Chem. Commun.* **1996**, 1673–1674.
- [17] See Supporting Information.
- [18] J. Huang, C. M. Haar, S. P. Nolan, W. J. Marshall, K. G. Moloy, *J. Am. Chem. Soc.* **1998**, *120*, 7806–7815.
- [19] G. P. Rosini, F. Liu, K. Krogh-Jespersen, A. S. Goldman, C. Li, S. P. Nolan, *J. Am. Chem. Soc.* **1998**, *120*, 9256–9266.
- [20] K. A. Woerpel, R. G. Bergman, *J. Am. Chem. Soc.* **1993**, *115*, 7888–7889.
- [21] M. J. Burn, M. G. Fickes, J. F. Hartwig, F. J. Hollander, R. G. Bergman, *J. Am. Chem. Soc.* **1993**, *115*, 5875–5876.
- [22] Y. Feng, M. Lail, K. A. Barakat, T. R. Cundari, T. B. Gunnoe, J. L. Petersen, *J. Am. Chem. Soc.* **2005**, *127*, 14174–14175.
- [23] The doublet $^{31}\text{P}\{^1\text{H}\}$ NMR signal of $[\text{Rh}(\text{N}_2)(\text{PNP})]$ at -60°C reproducibly shows a second doublet, shifted downfield by only 0.1 ppm, which we attribute to a second conformer (due to PNP rings and substituents) of $[\text{Rh}(\text{N}_2)(\text{PNP})]$.
- [24] J. N. Harvey, *Phys. Chem. Chem. Phys.* **2007**, *9*, 331–343.
- [25] R. Poli, *Chem. Rev.* **1996**, *96*, 2135–2204.
- [26] L. A. Watson, O. V. Ozerov, M. Pink, K. G. Caulton, *J. Am. Chem. Soc.* **2003**, *125*, 8426–8427.
- [27] A. Walstrom, M. Pink, X. Yang, J. Tomaszewski, M.-H. Baik, K. G. Caulton, *J. Am. Chem. Soc.* **2005**, *127*, 5330–5331.
- [28] CCDC-682087 contains the supplementary crystallographic data for this paper. These data can be obtained free of charge from The Cambridge Crystallographic Data Centre via www.ccdc.cam.ac.uk/data_request/cif.

Received: March 27, 2008
Published online: August 4, 2008